ELECTRICAL STIMULATION OF LIMBS PART III. JOINT POSITION CONTROL[a]

Alain Fournier

Laboratoire d'Automatique de Montpellier
Université de Sciences et Techniques du Languedoc
Place E. Bataillon, 34060 Montpellier-Cedex, France

Etienne Dombre

I.N.S.E.R.M. U 103 Unité de Recherches Biomécaniques
Avenue des Moulins, 34000 Montpellier, France

Philippe Coiffet

Laboratoire d'Automatique de Montpellier
Univesité de Sciences et Techniques du Languedoc
Place E. Bataillon, 34060 Montpellier-Cedex, France

INTRODUCTION

The physiological study of muscular contraction enables one to describe the mechanisms of nerve conduction (1), of synaptic transmission, of amplification performed by the motor end-plates (2), and of contraction of the motor-units (3). None of these descriptions enables one to obtain the mathematical relationships which represent the total behavior of the neuromuscular loop. In order to obtain a simple model, we chose an electromechanical representation of the process rather than a combination of the models developed from the study of the structure and the characteristics of each element.

This paper describes the modeling and the position-control of a single-degree-of-freedom joint by means of pulse-width modulation of the signal sent to the agonist muscle's nerve. The first part presents an experimental procedure devised from the previous results of this study (4,5). In the second part, the mathematical methods used in order to identify the process and to analyze the results obtained are concisely shown.

[a]Based on work performed under VA Contract V101 (134) P-132.

DYNAMIC STUDY OF A JOINT WITH A SINGLE DEGREE OF FREEDOM

Description of the Process

Measurements have been performed on ankles of anesthetized dogs. The tibia is maintained in a fixed horizontal position, and hence the paw revolves in a vertical plane around an axis fixed in space. Electrical stimulation of the external popliteal sciatic nerve produces contraction of the anterior tibialis, and thus dorsiflexes the paw. The forces involved during the contraction period are:

1. The muscular force developed during the contraction of the agonist muscle group;
2. The muscular force coming from the stretched antagonist muscle group which is not stimulated;
3. The passive effects of ligaments and mechanical limits of the joint;
4. The viscous damping forces, proportional to the rotational velocity; and,
5. The external load and the weight of the paw.

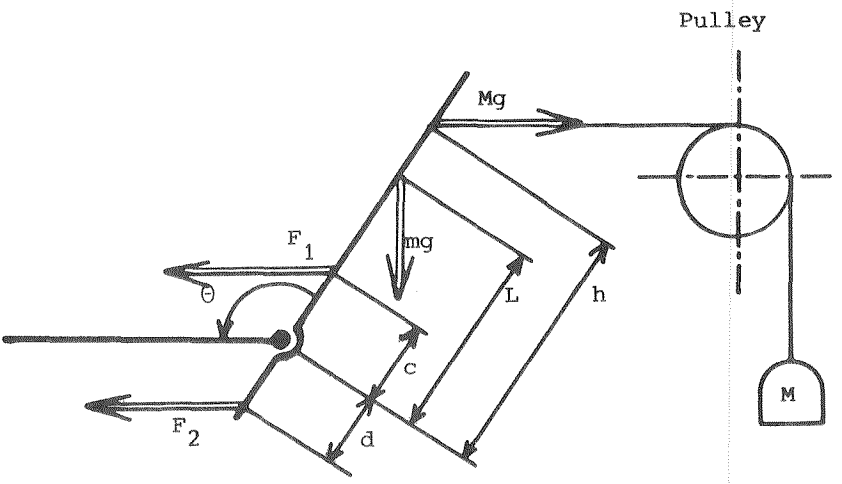

FIGURE 1. – Diagram of an ankle joint.

In order to write the equations of the dynamic system, let us consider a schematic diagram of an ankle joint (Fig. 1).[b]

[b] The diagram given in Part II, Figure 22, p. 286, BPR 10-22, is slightly different. For dogs, c and d are very small in comparison with the distances D_1 and D_2 shown in Figure 22, i.e., $\frac{c}{D_1} \sim \frac{d}{D_2} \ll 1$. Thus, F_1 and F_2 may be assumed to be parallel to the longitudinal axis of the tibia with negligible error.

The equation is:

$$J\frac{d^2\theta}{dt^2}=\left[dF_2 - cF_1 + Mgh\right]\sin\theta - mgL\cos\theta - \xi\frac{d\theta}{dt} \qquad [1]$$

where θ, F_1 and F_2 are the variables governing the motion; J, c, d, M, m, h, L, and ξ are biomechanical parameters; the physical parameters are J the moment of inertia, m the mass of the paw and of the position transducer together, and ξ the viscous damping coefficient.

Determination of the Biomechanical Parameters

Equation [1] shows physical terms which are not easy to measure and which we were unable to compute with sufficient accuracy.

Measurement of J is difficult. The "quick release" method (6) can be performed. Recording the period of oscillations of the free lever is another method of computing the moment of inertia (7, 8). Since these measurements need complex experiments for each subject, we chose to divide equation [1] by the moment of inertia J and to express the parameters as functions of the moment of inertia. Equation [1] then becomes:

$$\frac{d^2\theta}{dt^2}=\left[\frac{d}{J}F_2-\frac{cF_1}{J}+\frac{Mgh}{J}\right]\sin\theta-\frac{mgL}{J}\cos\theta-\frac{\xi}{J}\frac{d\theta}{dt} \qquad [2]$$

The coefficients c and d represent the distances between the center of rotation of the joint and the points where the forces developed by the agonist muscle group and antagonist muscle group, respectively, are applied. We tried to determine these distances by dissection of a dog's leg but accurate measurement was impossible because the tendon branches, and its area of insertion on the bone is wide, thus making the center of pressure difficult to define. The mass M of the external load is known with accuracy. However, the distance h between the center of rotation of the joint and the point of application of the wire transmitting the external force is inaccurate. The Mass m, of the paw and the position transducer together, and the distance L between the center of gravity of the paw and the joint center, cannot be measured directly. Computation of the viscous damping coefficent ξ from the decrease in the paw oscillations does not yield accurate results.

Among the variables governing the motion of the paw, only the joint angle can be directly measured during the experiment. It is very difficult to measure the force developed by the stimulated muscle and the passive

effects of the system without measurably altering the system.[c] It is thus necessary to proceed to other experiments in order to determine the unknown forces.

Determination of the Control Signal and of the Joint Position

The conditions of this experiment are shown in Figure 2.

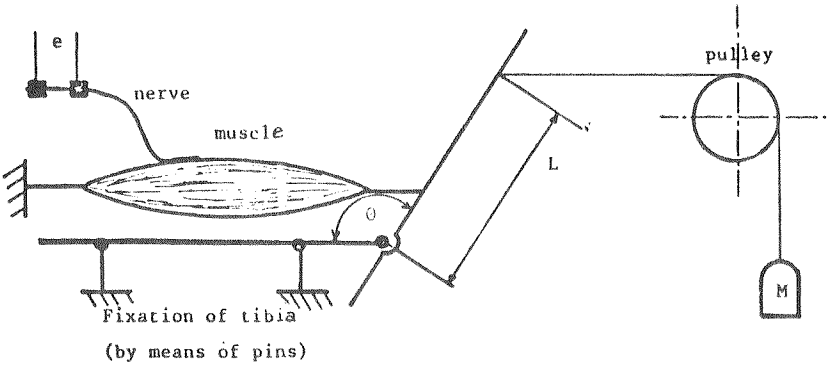

FIGURE 2. — Experimental procedure.

The stimulator delivers pulses with a fixed frequency and amplitude of 45Hz and 150mV respectively; control is achieved by pulse width modulation from 10μs to 4ms) of the stimulation signal. This signal is recorded as well as the joint position θ (Fig. 3).

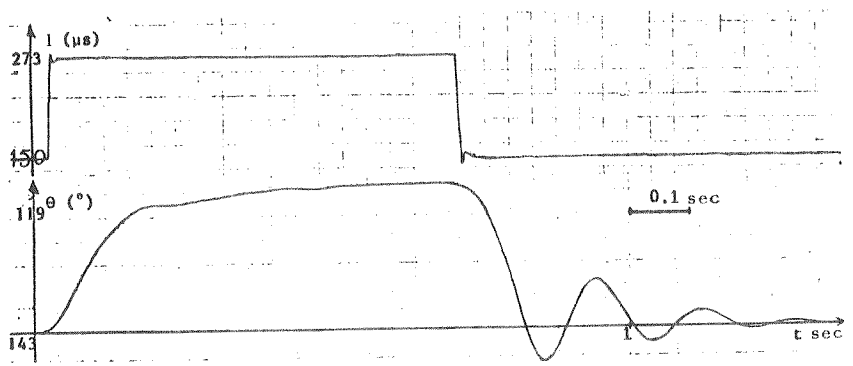

FIGURE 3. — Recordings of the input signal (pulse width l) and of the output signal (angular position θ) (BECKMAN DYNOGRAPH R.M.).

[c]The method of measuring the force developed by the stimulated muscle by implanting transducers in the muscle tendons as described in Part I, pp. 266-267, BPR 10-22, was abandoned because of the following difficulties encountered: 1. damage of tendons, 2. continual drift of output signals, and 3. malfunction of the fragile transducers.

The damped oscillations of θ, which are observed when the stimulation causes overshoot (corresponding with the return of the external load to its initial position) are due, at least in part, to the mechanical vibrations of the metallic frame designed to maintain the tibia in a stable and horizontal position. Tests have been performed with different external loads; the pulse-width of the stimulation signal has been adjusted in order to obtain the maximum rotation of the paw (about 30 deg).

Determination of the Antagonists' Passive Effects

Whereas the driving force depends on the stimulation signal, the antagonist forces are a function of the joint position only.

To determine the antagonists' resultant passive force F_{ANT}, the paw is manually rotated through its full range of motion from one mechanical

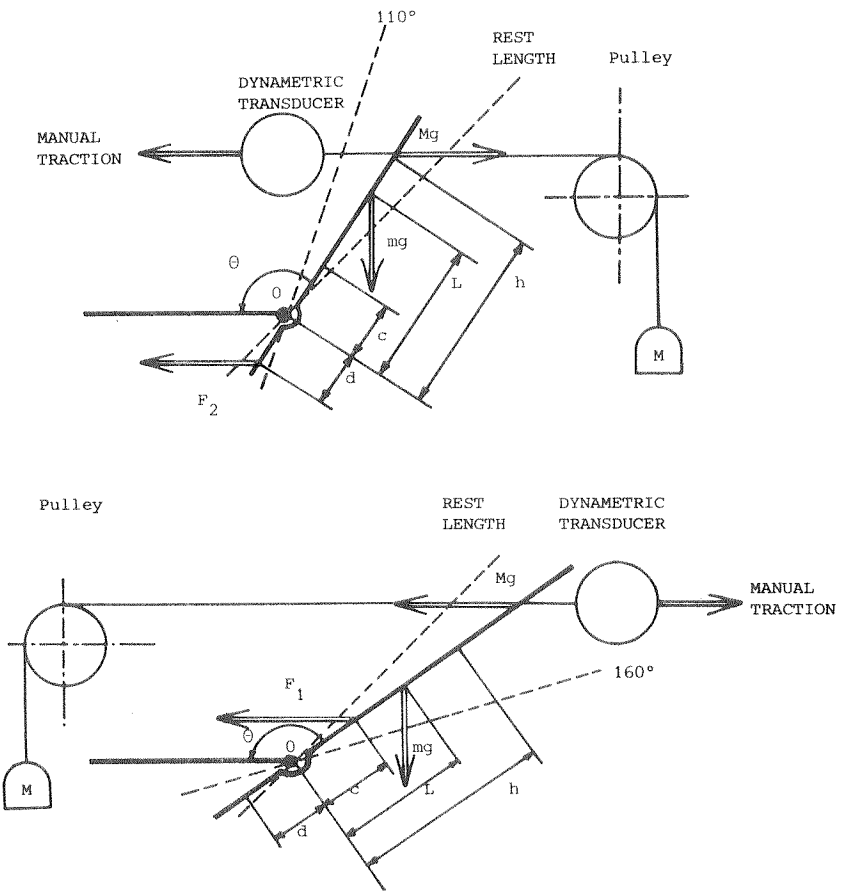

FIGURE 4.—Determination of the antagonists' effects.

limit of the joint to the other. Figure 4 shows the principle of the two experiments, θ being the axis of rotation. We have:

$$\text{Moment of } F_{ANT} = \begin{pmatrix} \text{Moment of force} \\ \text{from manual traction} \end{pmatrix} \pm (\text{Moment of mg}) - (\text{Moment of Mg})$$

The traction force on the dynamometer ring and the total angle of rotation are simultaneously recorded. The resulting curve, shown in Figure 5, is obtained after compensation for the gravity forces and allows one to determine the antagonists' effects as a function of the joint position θ.

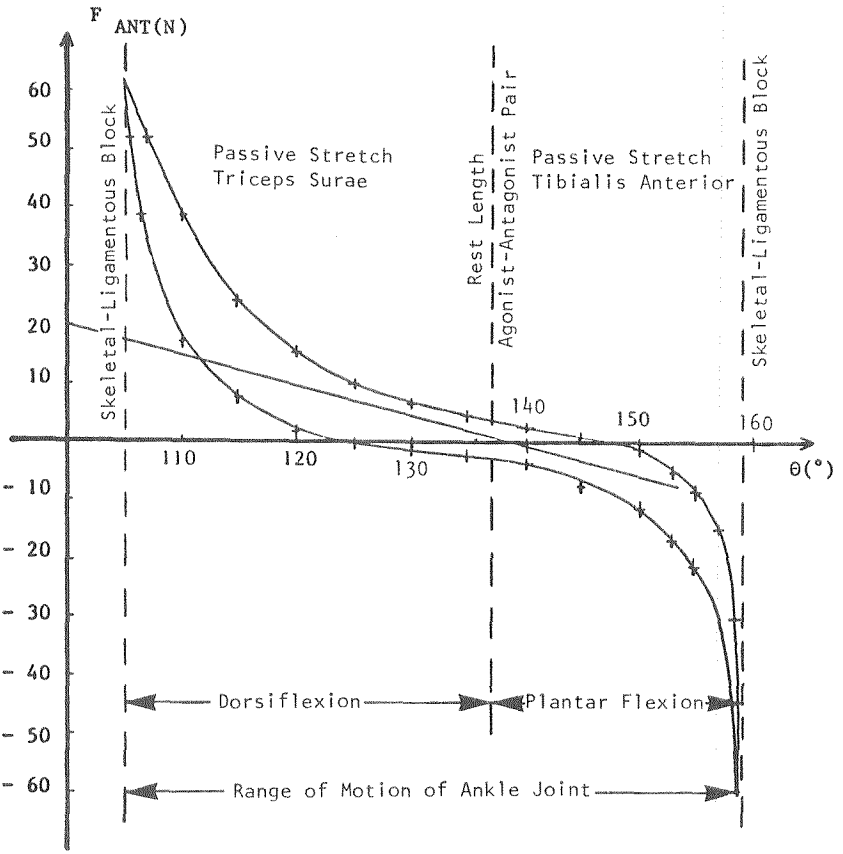

FIGURE 5. — Passive effects of F_{ANT} as a function of θ.

Determination of the Muscular Force

Any surgical operation on the tendon changes its characteristics. In an attempt to avoid any alteration of the neuromuscular system, we decided to wait until after the conclusion of the joint-position control experiment and then cut the tendon of the agonist muscle group. The experimental procedure followed is shown in Figure 6.

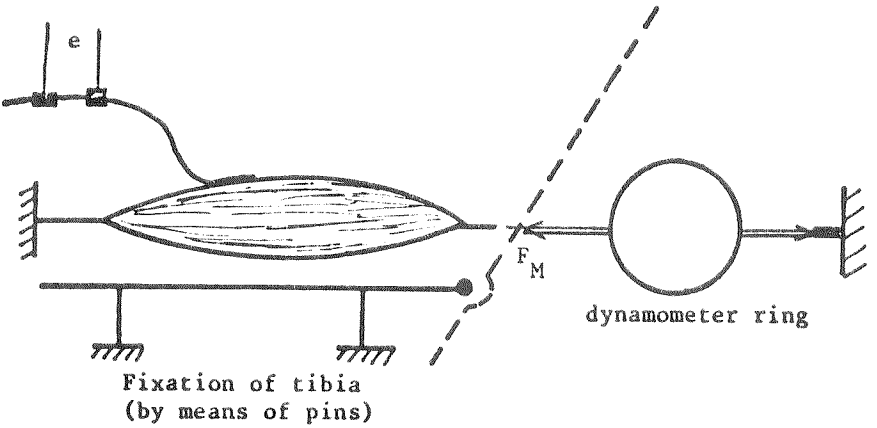

FIGURE 6. – Experimental procedure.

A dynamometer ring is set along the main axis of the muscle. Under identical stimulation conditions as in the first experiment, the isometric force developed by the stimulated muscle is recorded (Fig. 7). The relationship between the stimulation signal and the muscular force which is developed can then be characterized.

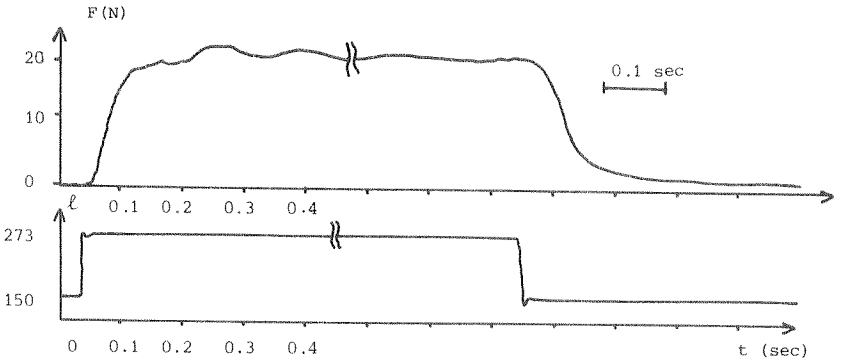

FIGURE 7. – Recordings of the force developed by the stimulated muscle and of the stimulation pulse width.

EXPERIMENTAL RESULTS

Characteristics of the Antagonists' Passive Effects

The curve $F_{ANT}(\theta)$ shown in Figure 5 allows one to verify the following points:

1. When the paw is in a position near rest length, the antagonist forces involved are small,
2. Near the extreme states, a locking appears, due to the stiffness of the ligaments and the mechanical limits of the joint.
3. Dorsiflexion and plantar flexion of the paw are characterized by an hysteresis effect. The branch of the cycle followed depends on the initial conditions and on the direction of the motion. It is incorrect to assume that the force $F_{ANT}(\theta)$ passes from one branch of the cycle to the other when little oscillations occur.

As a first approximation we have characterized the curve $F_{ANT}(\theta)$ by linear segments which represent the average behavior (Fig. 8).

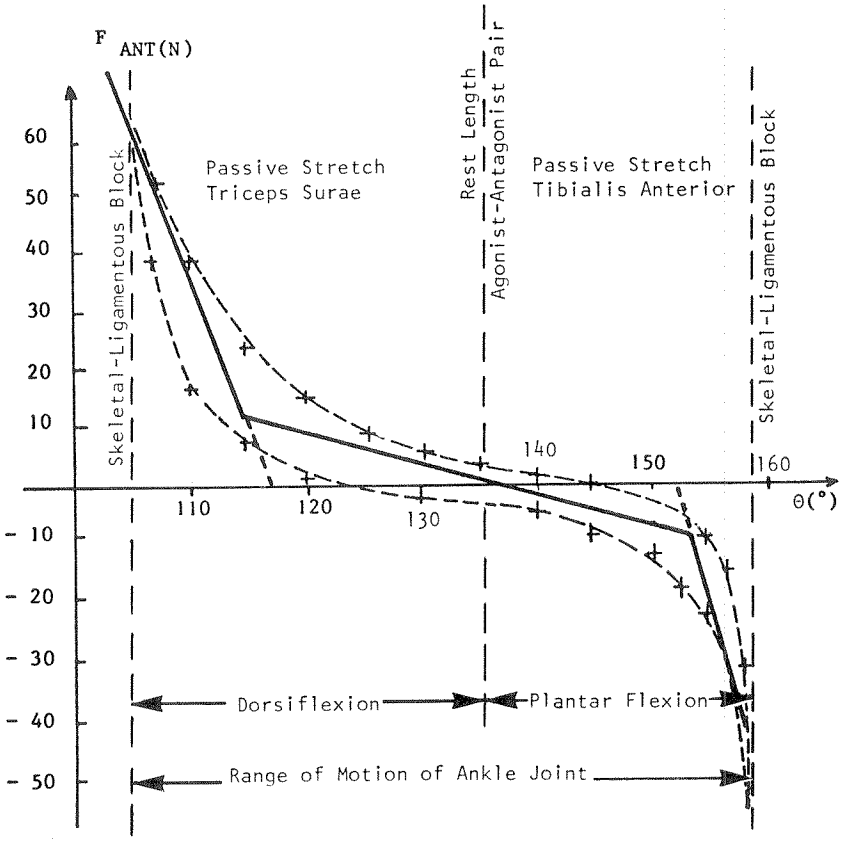

FIGURE 8. — Linearization of the antagonists' passive effects.

Characterization of the Muscular Force $F_1(t)$

The curves of Figure 7 show that the stimulated muscle behaves as a first-order system. A short delay time in the muscle's response can also be observed but will be neglected during the identification procedure. Muscular contraction appears when a certain threshold of pulse-width is exceeded (4). If the pulse width is large (>lms) a saturation effect can be observed. The electromechanical system may be represented by the block diagram shown in Figure 9, which includes the pulse width modulator, the nerve, and the muscle.

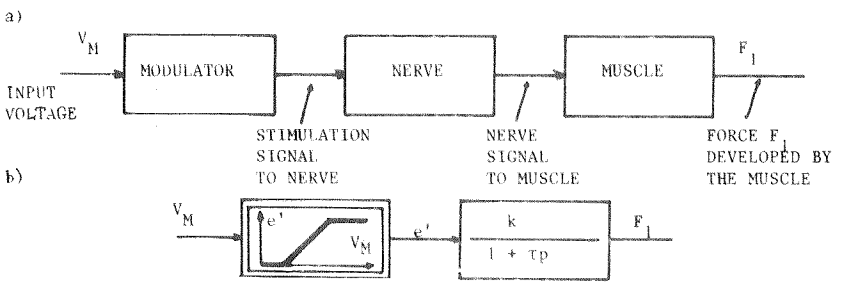

FIGURE 9.—Block diagram of the electromechanical system: a) physical representaion; b) equivalent block-diagram for the computation.

Characterization of the Joint

Let us consider the ankle joint with only the anterior tibialis as actuator. The process is then controlled by the driving muscular force. The output of the system is the joint position.

Equation [2] can be written as follows:

$$\frac{d^2\theta}{dt^2} = \left[k_2 (F_{ANT} + Mg) - k_1 F_1\right] \sin\theta - mg\, k_2 \cos\theta - k_3 \frac{d\theta}{dt} \qquad [3]$$

The antagonists' passive effects are brought back to the point where the external load is applied and this point can be assumed to have the same spatial location as the center of gravity of the paw, i.e., the distances h and L are nearly the same. The previous differential equation can be represented by the block-diagram shown in Figure 10.

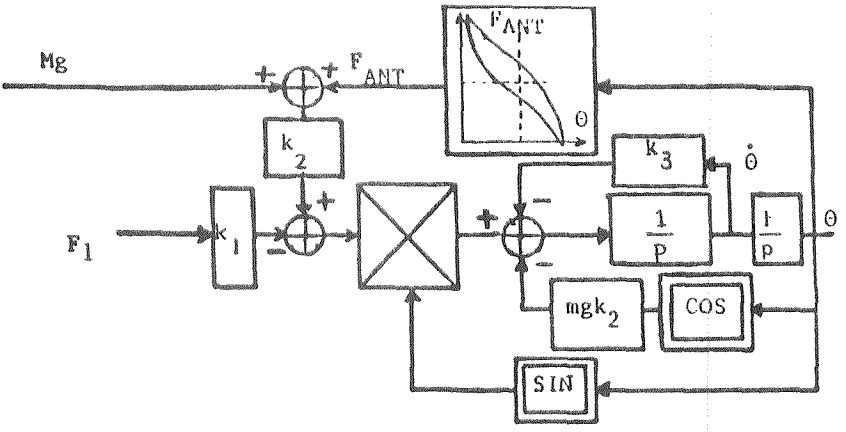

FIGURE 10. — Block diagram of the mechanical model of the joint.

IDENTIFICATION PROCEDURES

Model of Muscle Alone

We experimentally evaluated the threshold, the minimum pulse width with 150mV amplitude necessary to obtain the beginning of muscular contraction. Taking into account the good sensitivity of the dynamometer ring, this threshold has been obtained with accuracy. A supplementary study showed this factor to be a function of the state of fatigue of the muscle. In order to avoid the errors introduced by the fatigue factor, before every experiment we verified that the threshold value was equal to this initial value.

The effects of saturation have not been evaluated accurately since the value at which it occurs is always higher than the pulse width required.

The time delay observed between the application of the stimulation signal and the muscular contraction is shorter than the sampling period of the recorded signals. It, thus, could not be measured.

The first-order linear system, Figure 9, still remains to be identified; i.e., the values of gain K (N/μs) and the time constant τ (sec) still have to be estimated. To obtain K and τ, the method of linear estimation for a Kalman filter was used (9, 10).

Identification of The Joint

The model of the joint shown in Figure 10 is complex since it contains non-linear elements. To evaluate the parameters k_1, k_2, and k_3, the "Méthode du Modéle" (11, 12, 13) has been used. This method consists in searching in the parametric space for a point where E, the function of the error between the outputs of the process and the model, respectively, is a minimum (Fig. 11).

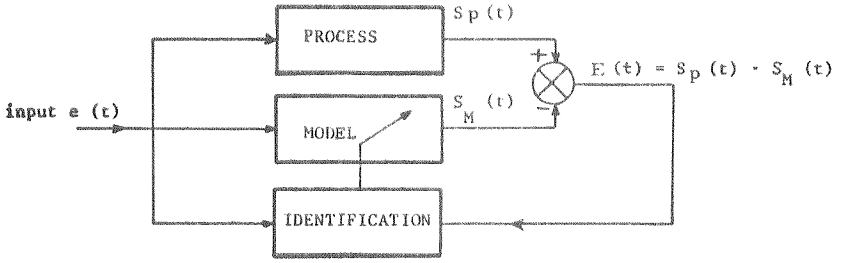

FIGURE 11.—Principle of the "méthode du modéle."

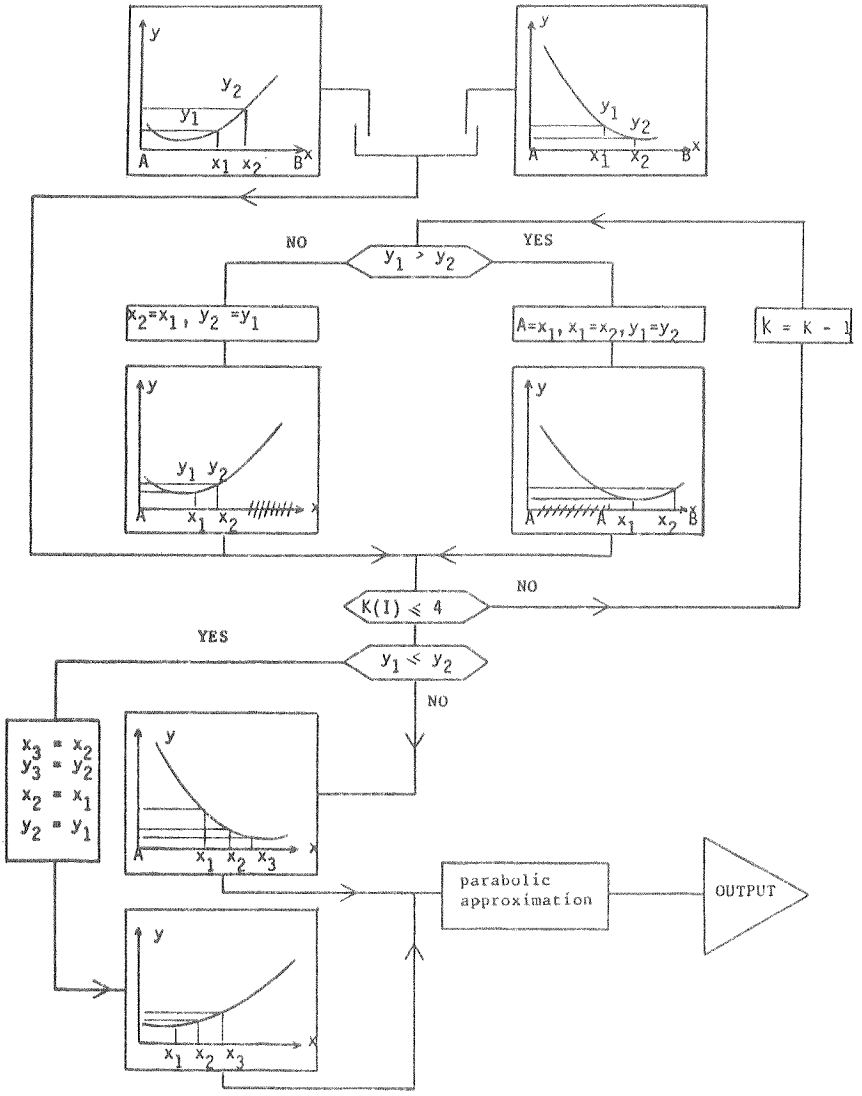

FIGURE 12.—Fibonacci's method: flow chart of the computation program.

This searching method in the parametric space may be executed in a random or an analytical manner; we chose Fibonacci's method which can be connected to a dichotomic method. However, this method requires the scale of sizes of the identified parameters to be known in order to define the searching area. The flow chart of the computation program is shown in Figure 12.

The results obtained by this method are satisfactory whenever the minimum of the function E is the only minimum in the searching area, and when all the parameters of the model are sensitized by the input of the process (i.e., a variation of the input produces a corresponding variation in each parameter). The recordings which are obtained are mixed with measurement and sampling noises. Therefore, the concept of absolute minimum is not realistic, and it is better to define an area of the parametric space over which the error of estimation, E, will be smaller than a fixed value of E_0 (Fig. 13). The evaluation of the "iso-error" surface for a given value of E_0 is obtained by computing the errors for points located around the nominal point determined by Fibonacci's method. In the searching process when a point lies outside of the "iso-error" surface, a linear interpolation with respect to the nominal point is performed. If some parameter is not well-sensitized, the model's output value varies in a large scale. If the error regions are small and if a non-empty region of intersection exists when several tests are considered, the proposed model is valid for those cases.

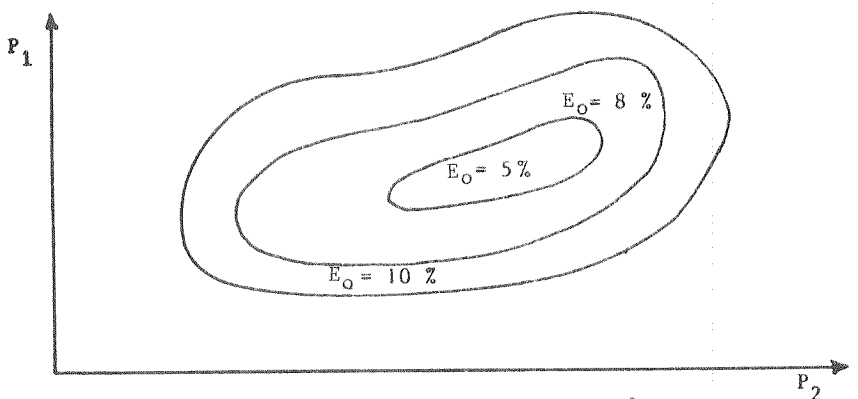

$$E = 100\% \times \frac{\int_s (\Theta_{actual} - \Theta_{model})^2 dt}{\int_s (\Theta_{actual} - \Theta_{average})^2 dt}$$

FIGURE 13.—Representation of the "iso-error" regions in a two-dimensional parametric space.

Simulation of the Model

The identification being completed, it is necessary to check the validity of the results obtained. The actual experimental process is run and then

using the same input values (voltage, amplitude, and pulse width), the model is simulated. The outputs are then compared—the actual measured value of θ and the calculated value of θ. Wherever the results are identical, it is possible to establish a control law from the model.

RESULTS OF IDENTIFICATION PROCEDURES

Identification of the Muscle Model

In two representative experimental trials, numbers 3-23 and 4-24 with external load, M, of 10N and 15N respectively, the nerve was excited by a series of pulses of modulated width, the width quickly increasing between two values. The lower value used, 150μs, is under the muscular contraction threshold of 180μs. The upper values used in trials 3-23 and 4-24 were 273μs and 332μs, respectively. The results of the identification procedure are given in Table 1.

From the experimental trials we selected average values for K and t of:

$$K = 0.65\ N/\mu s$$

$$\tau = 0.05 sec.$$

TABLE 1.—*Results of the Identification Procedure*

Test	Width (μs)	Gain K (N/μs)	Delay time τ(sec)
3-23	273	0.60	0.06
4-24	332	0.70	0.04

Identification of the Joint Model

The results of the previous electromechanical muscle model identification are used in the simulation of the agonist muscle's force. Table 2 shows the results obtained, the two previous trials are illustrated.

TABLE 2.—*Results of the Identification Procedure*
(Searching for the nominal point by Fibonacci's method; E denotes the estimation error at the nominal point obtained by Fibonacci's method)

Test	k_1	k_2	k_3	E
3-23	34	80	58.5	5.35
4-24	28	71.3	107	3.67

The error introduced in the identification procedure is acceptable as the errors introduced in the measurements of the physical variables are of greater significance. However, the values of the parameters used differ for different experimental trials. This requires that the "iso-error" regions be searched to show if a non-empty intersection exists for each parameter.

Tables 3 and 4 give the results obtained for 10 percent "iso-error" regions for trials 3-23 and 4-24, respectively. The regions of intersection for trial no. 3-23 are shown in Figure 14. The estimation error, E, of each point of the parametric space located in the intersection space is less than or equal to 10 percent. In view of the very limited accuracy of the physical measurements, it is not necessary to decrease the error requirements for the "iso-error" regions.[d]

TABLE 3—*Test No 3-23*

	Maximum	Minimum	Average
k_1	65.498	27.656	46.577
k_2	170.960	72.566	121.763
k_3	104.108	55.248	79.678

TABLE 4.—*Test No 4-24*

	Maximum	Minimum	Average
k_1	35.461	25.257	30.359
k_2	90.734	64.388	77.561
k_3	124.483	98.456	111.469

Simulation of the Total Model

Two models have, thus, been identified: the first one represents the neuromuscular loop, the second one represents the joint system. Simulation of these models in the same open loop permits their total behavior to be compared with that of the real processes described in the experiments performed in the "Dynamic Studies" in references 4 and 5. (The simulation block diagram is shown in Figure 15.) The effects of the antagonist muscles and the angular acceleration may also be included.

[d]The large range of values obtained for k_1, k_2, k_3, are not necessarily indicative of the accuracy of the model. The parameters of our model, K, τ, were found to be quite sensitive to the excitability threshold, the value of which, in turn, we were unable to measure accurately because of hardware problems. Rather than trying to reduce the confidence range of the parameters with one trial, we chose to search the intersection of the confidence ranges from numerous experiments.

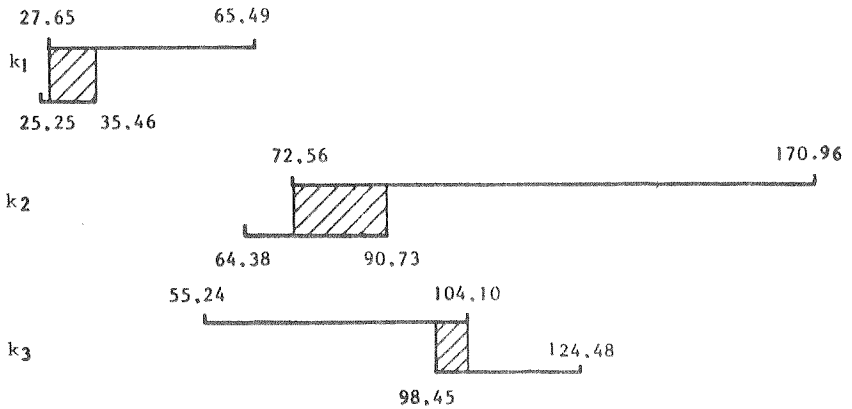

FIGURE 14. – Intersections of 10 percent "iso-error" regions: test no. 3-23.

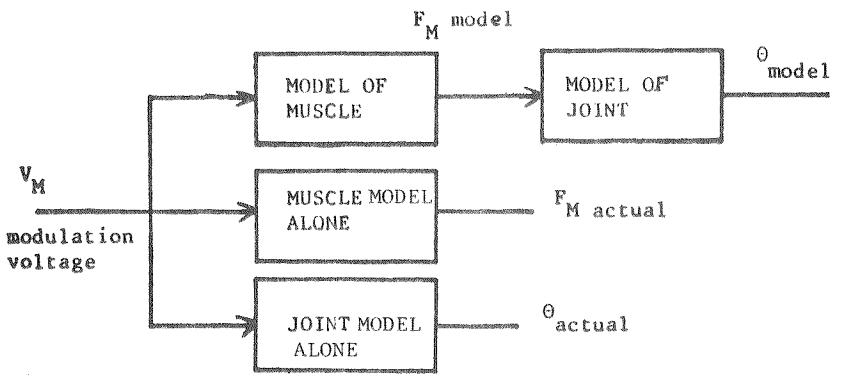

FIGURE 15. – Block diagram of the simulation of the total model and its respective parts.

Average values from the domains of intersection were used for the parameters:

1. Threshold of pulse-width, $S_0 = 180\mu s$;
2. Gain of the neuro-muscular loop, $K = 0.65 N/\mu s$;
3. Time constant of the neuro-muscular loop, $\tau = 0.06$ sec;
4. coefficient $k_1 = 32\ (kg\text{-}m)^{-1}$
5. coefficient $k_2 = 80\ (kg\text{-}m)^{-1}$
6. coefficient $k_3 = 83\ (kg\text{-}sec)^{-1}$

(k_1, k_2, k_3 are gains given in equation [3] page 13. They are a function of both the physical parameters of the system and the moment of inertia.)

Simulation of the neuromuscular loop using the previous values for the parameters K, τ, and S_ℓ shows a close comparison between the simulated muscular force and the measured muscular force, Figures 16 and 17.

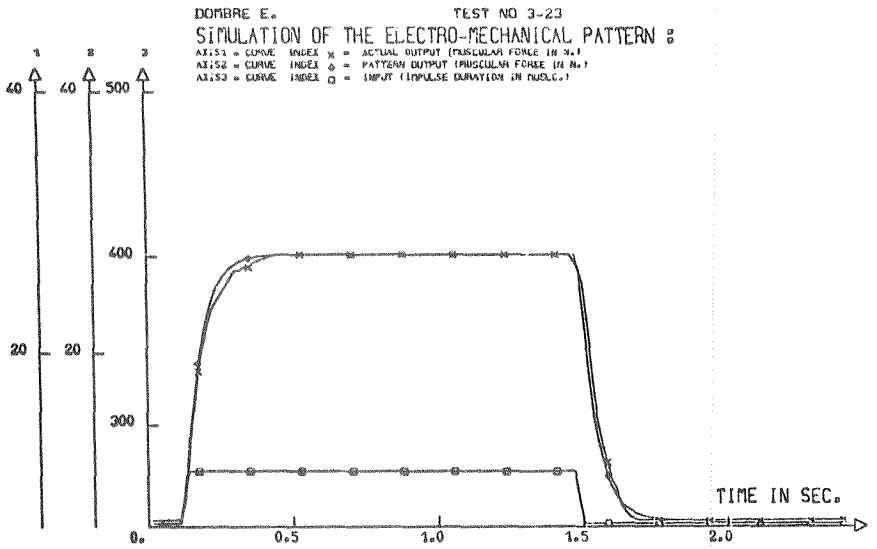

FIGURE 16.—Simulation of the electromechanical neuromuscular model: test no. 3-23. Curve index x = Actual Output (muscular force in N). Curve index ◇ = Model Output (muscular force in N). Curve index □ = Input (pulse width in μsec).

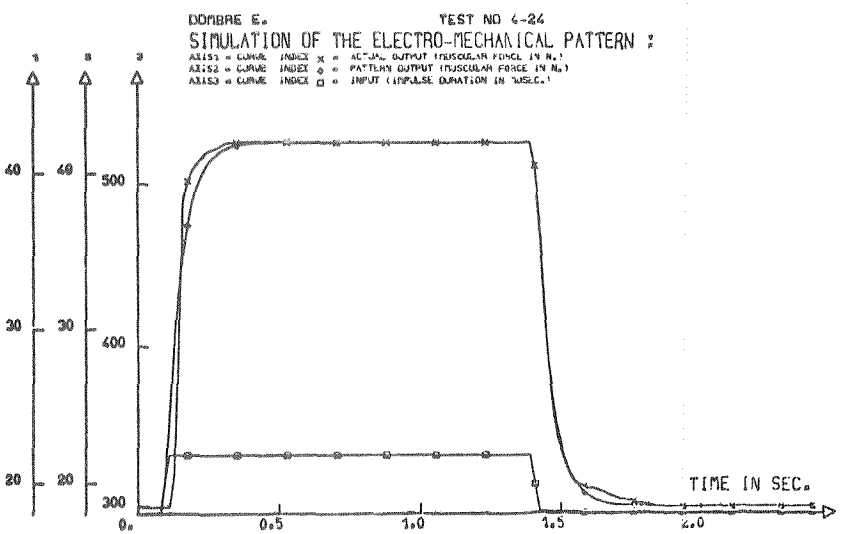

FIGURE 17.—Simulation of the electromechanical neuromuscular model: test no. 4-24. Curve index X = Actual Output (muscular force in N). Curve index ◇ = Model Output (muscular force in N). Curve index □ = Input (pulse width in μsec).

Figures 18 and 19 show the comparison of the output of the simulation of the complete model, simulated joint position, and the actual measured joint position.

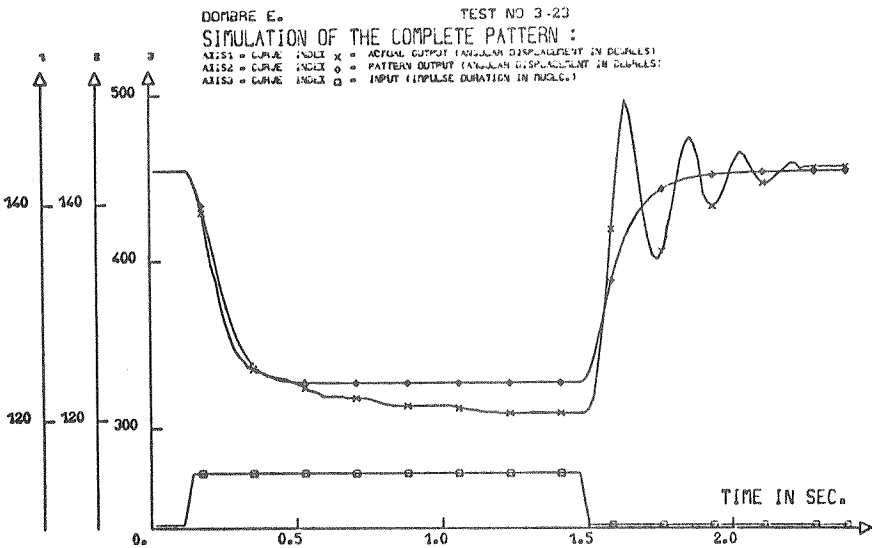

FIGURE 18.—Simulation of the complete model: test no. 3-23. Curve index X = Actual Output (angular displacement in degrees). Curve index ◇ = Model Output (angular displacement in degrees). Curve index □ = Input (pulse width in μsec).

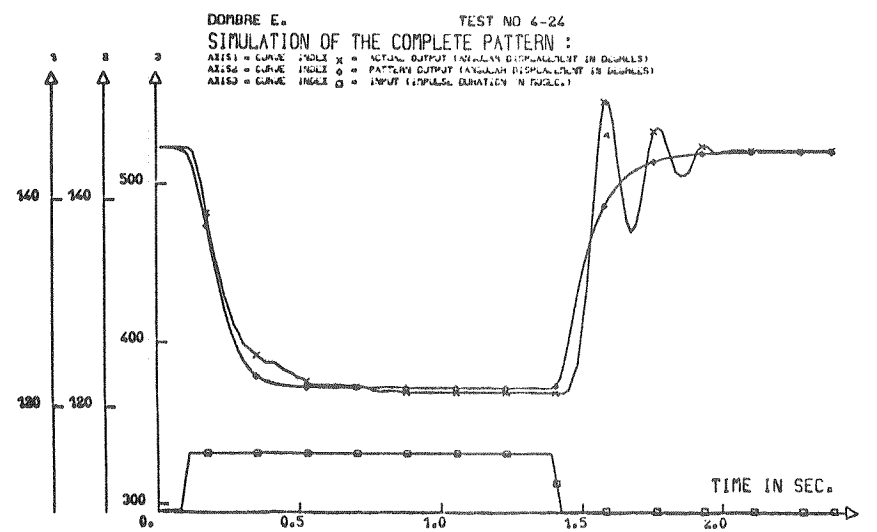

FIGURE 19.—Simulation of the complete model: test no. 4-24. Curve index X = Actual Output (angular displacement in degrees). Curve index ◇ = Model Output (angular displacement in degrees). Curve index □ = Input (pulse width in μsec).

The damped oscillations appearing in the curves of the actual outputs in Figures 18 and 19 arise from the mechanical vibrations of the metallic frame fastened to the operating table in order to maintain the tibia in a

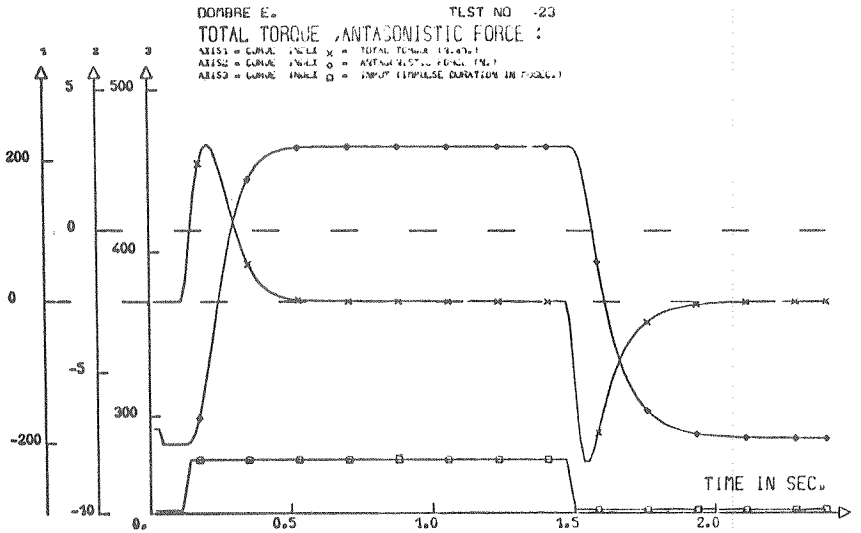

FIGURE 20. —Effects of the antagonist muscles and the angular acceleration: test no. 3-23. Curve index X = Total Torque (Nm). Curve index ◇ = Antagonist Force (N). Curve index □ = Input (pulse duration in μsec).

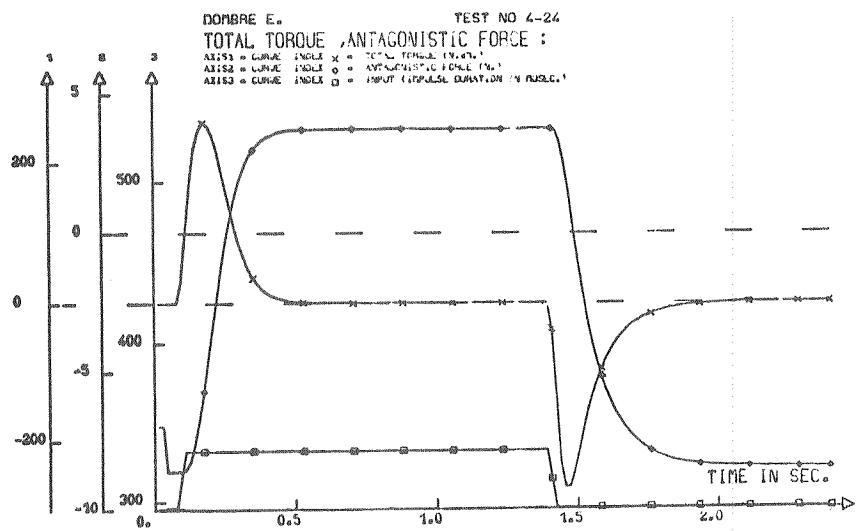

FIGURE 21. —Effects of the antagonist muscles and the angular acceleration: test no. 4-24. Curve index X = Total Torque (Nm). Curve index ◇ = Antagonist Force (N). Curve index □ = Input (pulse width in μsec).

fixed horizontal position. They do not appear in the simulated model. The steady states, during stimulation and when it is over, are identical in both the actual and simulated outputs.

Figures 20 and 21 show the simulated effects of the antagonist muscles and the angular acceleration.

CONCLUSION

The control law of a physical system must define a realistic mathematical model of the process and also provide a model simple enough to be useful. The proposed model satisfies these two criteria. The results of the simulation show that, with a single stimulation signal, the actual and the simulated outputs behave in an identical manner. Hence, the identification procedure has provided a sufficient estimation of the parameters of the system, thus obviating the necessity of determining biomechanical constants by complex and inaccurate measurements. Although progress yet remains to be made in the surgical area (e.g., in implantation of electrodes and achieving tolerance by the human body) we have defined the steps for the position control of an articulated system.

From the proposed model, it becomes possible to design an analog feedback control loop for a position servo-system and to stabilize the joint position when the external load is opposed to the agonist muscle's force. If the external load is variable, agonist and antagonist muscle groups of the joint have to be simultaneously involved. The previous identification procedure is still valid for each muscle group but problems of synergy of several muscular contraction effects arise. When the control of several coupled joints is considered, as in legged-locomotion problems, the logical level of synergy becomes more complex. A theoretical approach to these problems is being studied in our laboratory.

ACKNOWLEDGMENTS

The authors wish to express their gratitude to Professor P. Rabischong and E. Peruchon for useful discussions during this work. Also, they thank F. Bonnel for surgical assistance.

REFERENCES

1. Marx, C.: Le Neurone, Physiologie: Système Nerveux, Muscle. Charles Kayser, Tome 2, Chap. 1, p 7.
2. Lièvremont, M.: Contribution à l'Etude de la Jonction Neuromusculaire. Thèse d'État, Université de Paris, June 1972.

3a. Aubert, X.: Le muscle strié, Physiologie: Système Nerveux, Muscle. Charles Kayser, Tome 2, Chap. 19, p 1261.

b. Scherrer, J.: Physiologie de la Musculature Striée Squelettique chez l'Homme, Physiologie: Système Nerveux, Muscle. Charles Kayser, Tome 2, Chap. 20, p 1325.

4. Rabischong, P. et al.: Basic Studies in Electrical Stimulation of Limbs—Part 1.—Method and Approach. Bull. Prosthetics Res., 10-22, Fall 1974.
5. Rabischong, P. et al.: Basic Studies in Electrical Stimulation of Limbs—Part 2.—Open Loop Control of Muscular Contraction. Bull. Prosthetics Res., 10-22 Fall 1974.
6. Pertuzon, E.: La Contraction Musculaire dans le Mouvement Volontaire Maximal. Thèse d'État, Université des Sciences et Techniques de Lille, June 1972.
7. Dombre, E.: Commande en Position d'un Levier Squelettique par Stimulation Nerveuse. Thèse de 3e cycle, Montpellier, Mar. 1975.
8. Drillis, R., R. Contini, M. Bluestein: Body Segment Parameters. Artificial Limbs, 8(1):44-66, Spring 1969.
9. De Larminat, P.: Sur l'Identification par filtrage non linéaire, These d'État, Université de Nantes, May 1971.
10. Nahi, N.E.: Estimation Theory and Applications. John Wiley and Sons, New York 1969.
11. Richalet, J., A. Rault, and R. Pouliquen: Identification des Processus par la Méthode du Mòdele. Gordon and Breach, 1971.
12. Graupe, D.: Indentification of Systems. Van Nostrand Reinhold Co., New York 1972.
13. Bellman, R.E. and S.E. Dreyfus: Applied Dynamic Programming. Princeton University Press, Princeton, N.J. 1962.
14. Gugič, P., A. Trnkoczy, and U. Stanič: Hybrid Control of the Ankle Joint. Proceedings of the Fourth International Symposium on External Control of Human Extremities, Dubrovnik, pp. 617-631, Aug. 1972.
15. Liegeois, A. and A. Fournier: Modélisation et Commandabilité de la Locomotion Artificielle. Symposium sur l'Identification des Systemes Dynamiques Humains dans les Processus Homme-Machine, Lille, May 12-15, 1975.